Analysis of Frequency Chirping of Optical Phase Conjugate Signals by Four-Wave Mixing in Light-Holding SOA's

Jyh-Tsung Hsieh, Pei-Miin Gong, San-Liang Lee, and Jingshown Wu, *Member, IEEE*

***Abstract*—We propose to use an additional injection beam of short wavelength to enhance the wavelength conversion that utilizes the four-wave-mixing (FWM) effect in a semiconductor optical amplifier (SOA). With this scheme, an assist light can increase the saturation intensity without sacrificing the gain of a SOA, and this leads to an increase in conversion efficiency. A numerical method dealing with FWM, amplified spontaneous emission noise, longitudinal spatial hole burning, wavelength dependent gain spectrum is developed to predict the static and dynamic characteristics of our scheme. The effects of holding light on extinction ratio and chirp dynamics are analyzed in detail. High-pump and/or low-signal power is shown to be effective in maximizing extinction ratio and minimizing peak frequency chirp.**

***Index Terms*—wavelength conversion, holding light, four-wave mixing, semiconductor optical amplifiers, extinction ratio, frequency chirp.**

I. Introduction

THE USE of the nonlinear mechanism of semiconductor optical amplifiers (SOA's) in advanced communication systems has been growing rapidly in recent years. One of the mechanism to be exploited for wavelength conversion is four-wave mixing (FWM). The wavelength conversion by virtue of the FWM process in SOA offers advantages such as multiwavelength conversion capability [1], transparency to the modulation format and data rate, and fiber dispersion compensation and so on. However, this technique suffers from low conversion efficiency and signal degradation caused by the amplified spontaneous emission (ASE) noise in the devices.

To raise the FWM conversion efficiency in SOA's, ultrafast relaxation-related gain process is dominant. As a rule of thumb, $\eta_{\max} \propto G_0 \cdot P_{sat}^2$ [2] is a good measure to obtain high FWM conversion efficiency [3]. G_0 is the unsaturated gain and P_{sat} is the saturation power of a SOA. In general, increasing the gain and/or saturation power will enhance the conversion efficiency. The fact that P_{sat} is inversely proportional to the carrier lifetime will in turn make it necessary to speed up the carrier recovery rate of a SOA.

A novel device termed as light-holding SOA (LHSOA) here has been proposed to alter gain characteristics and improve carrier dynamics through the injection of external assist light [4]. By setting the assist-light wavelength toward the transparency wavelength, the saturation power will increase without sacrificing the gain [4],[5]. We have demonstrated experimentally [6] that the saturation intensity and FWM wavelength conversion efficiency of a SOA could be raised with an assist light. The conversion efficiency can be enhanced by larger than 5 dB when the SOA is biased at transparency for a 23-dBm and 1480-nm assist light.

In this paper, a large-signal dynamic analysis for LHSOA was performed to calculate converted optical pulse waveforms and chirp by self-consistently solving the quasi-steady-state coupled equations and rate equations. Also, the effects of introducing an assist light are investigated. We calculate frequency chirping by considering the extinction ratio, the α-parameter along the longitudinal direction, and ASE noise. This may help in understanding and designing LHSOA's.

The structure of the paper is as follows. In Section II, the large-signal dynamic models based on FWM coupled equations and rate equations are described in detail. In Section III, we put emphasis on the performance assessment of the SOA with the injection of an assist light. Section IV deals time-domain analysis on extinction ratio and frequency chirping of conjugated signals using our time-developed model. Finally, conclusions are given in Section V.

II. Modeling FWM in SOA's

We have developed a numerical model to analyze the static and dynamic characteristics in LHSOA's. The model is based on position-dependent rate equations for the carrier density and the optical propagation equations in both directions for the whole spectrum of ASE and injected signals. Therefore, the model accounts for a nonuniform carrier distribution and can solve both below and above threshold conditions. The model

Manuscript received January 25, 2003. This work was supported in part by the National Science Council and the Ministry of Education, Taiwan, R.O.C. under Grant NSC91-2215-E-011-001 and 89E-FA06-2-4-7.

J. T. Hsieh is with the Graduate Institute of Communication Engineering and Department of Electrical Engineering, National Taiwan University, Taipei, 106 Taiwan, R.O.C. (phone: 886-2-2364-8318; fax: 886-2-2364-8318; e-mail: jyh_tsung@ pchome.com.tw).

P. M. Gong and S. L. Lee are with Department of Electronic Engineering, National Taiwan University of Science and Technologies, Taipei, 106 Taiwan, R.O.C. (e-mail: sanlee@et.ntust.edu.tw).

J. Wu is with the Graduate Institute of Communication Engineering and Department of Electrical Engineering, National Taiwan University, Taipei, 106 Taiwan. R.O.C. (e-mail: jingshownwu@ee.ntu.edu.tw).

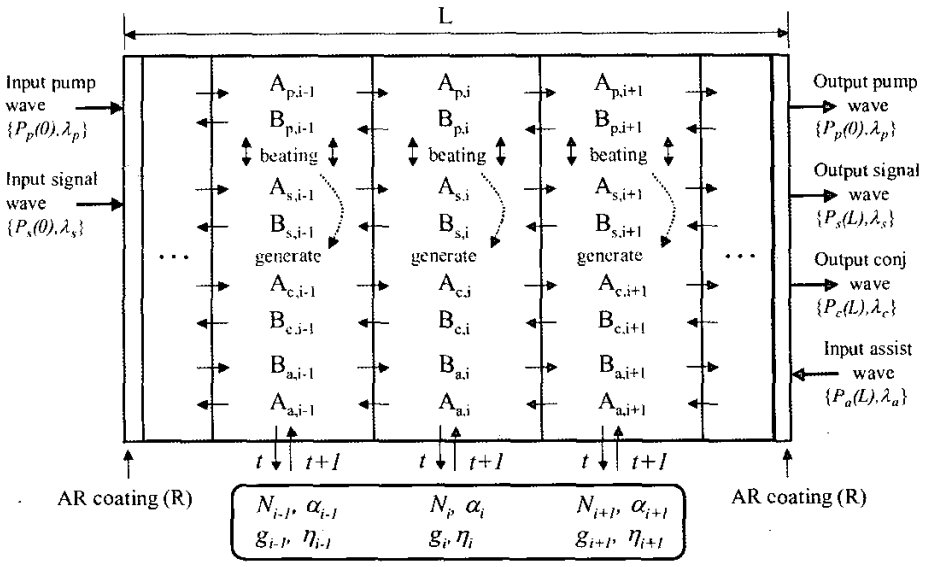

Fig. 1. Schematic diagram of the time-developed large-signal dynamic SOA model.

further includes a phenomenological expression for the total loss coefficient in the active layer, which explains the carrier relevant loss mechanisms. In addition, we also take into account both the spectral dependence and the carrier density dependence of the material gain to obtain a wavelength-dependent transparency. Fig. 1 shows a schematic of our static and dynamic large signal SOA model. The SOA is assumed to have negligible reflectivity at the end facets, and therefore only the forward-traveling waves exist.

To account for the interaction between carrier density N and photon density S, we divide the SOA into a number of small sections and solve the rate equation in each section. The carrier density $N_i(t)$ in section i of each SOA at time t is evaluated by the rate equation

$$\frac{dN_i}{dt} = \frac{J}{ed} - R(N_i) - \sum_{\omega} \Gamma v_g g_{i,\omega} S_{i,\omega} \tag{1}$$

where J is he current density, e is the electron charge, d is the active region thickness, Γ is the confinement factor, g is the material gain, S is the average photon density, and the index ω corresponds to different input light – pump, signal or conjugate. The average photon density $S_{\omega,i}$ is calculated by

$$S_{\omega,i} = \frac{|A_{\omega,i}|^2 + |A_{\omega,i+1}|^2}{2v_g} \tag{2}$$

where $A_{w,i}$ is the forward-traveling wave amplitude.

The spontaneous recombination rate depends on the carrier density and is given by Equation (3)

$$R(N_i) = AN_i + BN_i^2 + CN_i^3 \tag{3}$$

where A is the unimolecular recombination constant caused by trapping sites. B is the bimolecular spontaneous radiative recombination coefficient and C is the Auger recombination coefficient. The spontaneous carrier lifetime τ_{si} is equal to $(A + BN_i + CN_i^2)^{-1}$. The effective carrier lifetime τ_{ei}, which induces contributions from both the spontaneous, stimulated recombination and ASE, indicates how fast the carrier density can be modulated and can be expressed by [7]

$$\frac{1}{\tau_{ei}} = \frac{1}{\tau_{si}} + v_g \cdot \frac{g_{mi}L_i + 1}{g_{mi}L_i} \cdot \frac{dg(N_i,\lambda)}{dN} \cdot S_{out,i} \tag{4}$$

where $S_{Out,i}$ is the total photon density of the SOA given by the stimulated emission and the ASE.

In order to model the asymmetric gain profile, the gain spectrum is assumed to be cubic and the material gain is approximated by [8]

$$g_{mi}(N_i,\lambda_\omega) = \frac{a_1(N_i - N_0) - a_2(\lambda_\omega - \lambda_N)^2 + a_3(\lambda_\omega - \lambda_N)^3}{1 + \varepsilon(S_{1,i} + S_{2,i})} \tag{5}$$

where a_1, a_2, and a_3 are gain constants, N_0 is the carrier density at transparency, and λ_N is the peak wavelength, which is assumed to shift linearly with the carrier density), and ε is the gain compression factor. We set the value of λ_N at 1550 nm in the absence of any light into the SOA. The material loss coefficient α_{ai} (m^{-1}) is modeled as a linear function of carrier density $\alpha_{ai}(n) = K_0 + \Gamma K_1 n_i$ [9], K_0 and K_1 are the carrier-independent and carrier-dependent absorption loss coefficients, respectively. K_0 represents the intrinsic material loss. K_1 is mainly due to intervalence band absorption. The net gain is given by [10] as

$$g_i = \Gamma(g_{mi} - \alpha_{ai}) - (1-\Gamma)\alpha_c - \alpha_{scat} = \Gamma g_{mi} - \alpha_{0i}. \tag{6}$$

where α_{0i} is the total internal loss.

Provided that the input waves are linearly polarized in the same direction, the quasi-steady-state evolution of the pump, signal, and conjugate wave amplitudes A_i, $i=p, s, c$ is given by the coupled equations [11]

$$\frac{dA_s}{dz}=\frac{1}{2}[\{\Gamma g_{mi}(1-i\alpha_i)-\alpha_{0i}\}-\Gamma g_{mi}(\eta_{sp}|A_p|^2+\eta_{sc}|A_c|^2)]A_s$$
$$-\Gamma\frac{g_{mi}}{2}[\eta_{pc}A_p^2A_c^*e^{-i\Delta\omega z}] \quad (7)$$

$$\frac{dA_p}{dz}=\frac{1}{2}[\{\Gamma g_{mi}(1-i\alpha_i)-\alpha_{0i}\}-\Gamma g_{mi}(\eta_{ps}|A_s|^2+\eta_{pc}|A_c|^2)]A_p$$
$$-\Gamma\frac{g_{mi}}{2}[(\eta_{sp}+\eta_{cp})A_sA_cA_p^*e^{i\Delta\omega z}] \quad (8)$$

$$\frac{dA_c}{dz}=\frac{1}{2}[\{\Gamma g_{mi}(1-i\alpha_i)-\alpha_{0i}\}-\Gamma g_{mi}(\eta_{cs}|A_c|^2+\eta_{cp}|A_p|^2)]A_c$$
$$-\Gamma\frac{g_{mi}}{2}[\eta_{ps}A_p^2A_s^*e^{-i\Delta\omega z}] \quad (9)$$

where $g(z)=g_0/(1+P(z)/P_s)$ is the saturated gain coefficient, g_0 is the small-signal gain coefficient, P_s and α are the saturation power and the linewidth enhancement factor of SOA induced by carrier density modulation, $P(z)=\sum_{i=p,s,c}|A_i(z)|^2$ is the total optical power inside the amplifier.

The FWM coupling coefficients η_{ij}, $i,j=p,s,c$ are given by

$$\eta_{ij}(z)=\frac{(\frac{1-i\alpha}{P_s})}{1+\frac{P(z)}{P_s}-i(\omega_i-\omega_j)\tau_1}+\sum_{m=2}^{3}\frac{(\frac{1-i\alpha_m}{P_{sm}})}{1-i(\omega_i-\omega_j)\tau_m}. \quad (10)$$

which contains three relaxation-related gain mechanisms [11], carrier density modulation (CM), carrier heating (CH), and spectral hole burning (SHB). The relaxation lifetimes are given by τ_m, (m=1,2,3) for carrier modulation, heating, and hole burning, respectively. The saturation power (P_{sm}) and linewidth enhancement factor (α_m) are given for each processes.

The ASE power $P_{ASE,k}$ at optical frequency ω within the bandwidth $\Delta\omega$ at the output of the kth section is given by [12]

$$P_{ASE,k}(\omega)=G_k(\omega)P_{ASE,k-1}+\hbar\omega\cdot\frac{\Delta\omega}{2\pi}\cdot n_{sp}$$
$$\cdot[G_k(\omega)-1](\frac{g(N_k,\omega)}{g(N_k,\omega)-\gamma_{sc}}). \quad (11)$$

where n_{sp} is the spontaneous emission factor given by $n_{sp}=\overline{N}(z)/(\overline{N}(z)-N_0)$ [13]. The first term in (11) represents the amplification of the ASE noise from the previous section, while the second term is the ASE noise generated within the kth section itself.

By calculating the rate equation numerically in each section i we can obtain the carrier density N_i from which the gain g_i and the refractive index n_i are determined. Incrementing the model in time involves first updating the wave amplitudes at the section boundaries. The updating procedure involves first resolving the coupled equations and this is followed by the traveling-wave amplitudes E_k at the subsection boundaries being updated. The subsection carrier densities N_i are then updated using Euler's solution of the time-dependent carrier conservation equation. The time t is then incremented by Δt, and the whole cycle is repeated.

Typical buried-heterostructure (BH) SOA operating in the 1.55 μm is considered for our simulation. Table I shows the simulation and device parameters used in our simulation and nonlinear (FWM) SOA parameters are summarized in Table II.

TABLE I
DEVICE AND MATERIAL PARAMETERS

Symbol	Description	Value	Unit
L	SOA length	1000×10^{-6}	m
w	Active layer width	1.5×10^{-6}	m
d	Active layer thickness	0.18×10^{-6}	m
A	Unimolecular recombination constant	1×10^{8}	s^{-1}
B	Bimolecular recombination constant	2.5×10^{-17}	m^3/s
C	Auger recombination constant	9.4×10^{-41}	m^6/s
a_1	Material gain constant	2.5×10^{-20}	m^2
a_2		7.4×10^{18}	m^{-3}
a_3		3.0×10^{-32}	m^4
a_4		3.155×10^{25}	m^{-4}
N_0	Carrier density at transparency	1.1×10^{24}	m^{-3}
λ_0	Wavelength at transparency	1595×10^{-9}	m
v_g	Group velocity	7.5×10^{7}	m/s
dn/dN	Differential refractive index	-1.2×10^{-26}	m^3
α_c	Loss in claddings	20×10^{2}	m^{-1}
α_{scat}	Scattering loss	10×10^{2}	m^{-1}
β	Spontaneous coupling factor	2×10^{-5}	--
I	Injection current	105×10^{-3}	A

TABLE II
NONLINEAR (FWM) SOA PARAMETERS

Symbol	Description	Value	Unit
$P_{sat,CH}$	CH induced power saturation	0.69	W^{-1}
$P_{sat,SHB}$	SHB induced power saturation	25.5	W^{-1}
α_{CM}	Linewidth enhancement factor by CM	3.2	--
α_{CH}	Linewidth enhancement factor by CH	3.6	--
α_{SHB}	Linewidth enhancement factor by SHB	-24.5	--
τ_{CH}	Carrier heating time	650×10^{-15}	s
τ_{SHB}	Spectral hole burning time	50×10^{-15}	s

III. STATIC CHARACTERISTICS

In this section, we explore the effects of introducing an assist light in SOA's as well as analyze the dependence of the conversion efficiency on input pump power, input signal power and wavelength detuning in a LHSOA.

A. Output Saturation Power

As we have mentioned above, the limited speed remains as a problem in SOA-based wavelength converters. The use of a holding light at transparency will maintain the separation of the quasi-Fermi levels and enhances the gain recovery time. The assist light is transparent in the steady state ($g_a=0$), and has negative gain after signal pulse is amplified ($g_a<0$). As long as the assist light term of *Eq.* (1) is negative, i.e., $g_aP_a<0$, the recovery time becomes shorter than τ_s. Moreover, a larger power P_a gives a shorter recovery time.

On the other hand, it is known that gain saturation intensity is nearly in inverse proportion to the carrier lifetime of SOA's. Therefore, this light injection method is expected to improve

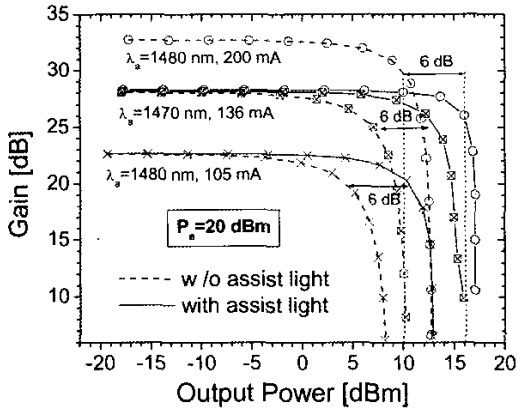

Fig. 2. Comparison of gain versus output power of an SOA for a 1550-nm signal between the absence and presence of an assist light. The solid and dashed curves represent the gain with and without an assist light.

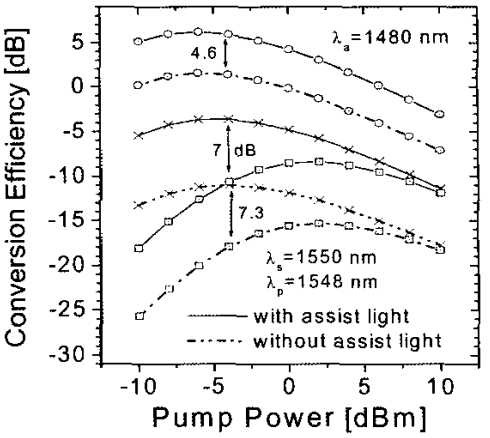

Fig. 3. FWM conversion efficiency of a SOA under the conditions with and without an assist light. The solid and dashed lines represent 'with' and 'without' the injection of an assist light, respectively. Circles: P_a=200 mA, P_s=-10 dBm; Crosses: P_a=105 mA, P_s=-10 dBm; Squares: P_a=105 mA, P_s=-3 dBm.

the saturation characteristics as well. The gain saturation characteristic of the SOA at different biases is shown in Fig. 2, where chip gain is plotted as a function of signal output power at the facet. Circles and Crosses plot the gain with and without pumping light injection, respectively. The holding light injection improves the saturation output power by 6 dB without reducing the unsaturated gain. The improvement of the gain saturation is also observed at a different bias current of 200 mA. In this case, the improvement in gain saturation is accompanied by a reduction in the unsaturated gain.

B. Conversion Efficiency

Fig. 3 shows the calculated conversion efficiency as a function of the input pump power for different signal power without and with a holding light of 20 dBm power, and the wavelength shift of 4 nm. The conversion efficiency is defined as the ratio of the output conjugate signal power to the input signal power. The conversion efficiency is changed by interaction between input powers and gain saturation. With increasing pump powers, the conversion efficiency is increased, because it is proportional to gain and the square of the pump power. However, with further increase of pump power, the conversion efficiency is decreased due to passing through the strong gain saturation region of the conjugate wave.

It's clearly seen from this figure that the conversion efficiency has been largely improved with the injection of a holding light. The effective carrier lifetime is reduced by introducing a holding light, and in turn extends the output saturation power of the SOA. Improved FWM conversion efficiency is thus benefited from these advantageous effects.

IV. Dynamic Characteristics

In this section, we analyze the dynamic characteristics of the LHSOA using our numerical model. As it's well known, extinction ratio and frequency chirping are very important parameters to determine transmission performance of conjugate signal. We thus performed further investigation on parasitic frequency chirp and extinction ratio of conjugate signal. Super Gaussian pulses (m=3) and a 2^7-1 pseudorandom bit sequence (PRBS) data pattern are used in our simulation as the input signal power. The frequency chirp $\Delta\nu$ of the output signal can be defined as $\Delta\upsilon = \frac{-1}{2\pi}\frac{d\phi}{dt}$, where ϕ is the phase of the output optical field.

A. Frequency Chirping of Conjugate Waves

Fig. 4 shows (a) the simulated output conjugate pulse patterns and (b) their associated frequency chirp for FWM in a LHSOA biased at 200 mA with and without an assist light. For the sake of demonstration, the input data rate is 2.5 Gb/s. However, the model makes no matter to apply up to data rate of 40 Gb/s.

The conjugate signal undergoes overshoot on the rising edge and a little undershoot on the falling edge. This is caused by the fact that the photon lifetime is significantly shorter than the carrier lifetime. From these figures, we found that the spectral inversion of conjugate signal resulted from the phase conjugation. Using this effect, it is possible to perfectly compensate for signal distortion by GVD and SPM on optical transmission. We note that the fluctuation of the converted signal is reduced as the pump light power increases. In Fig. 4(b), the variation of the frequency chirp is reduced similar to that of the pulse shape, that is to say, the frequency chirp is directly related to gain fluctuation [14].

By setting the injection current at transparency (I=105 mA), a similar result is obtained. The chirp fall and rise times are significantly shorter for the amplifier with a holding light. Compared to the results in Fig. 4, we can identify that the rise and fall times for both the conjugate and the chirp increase,

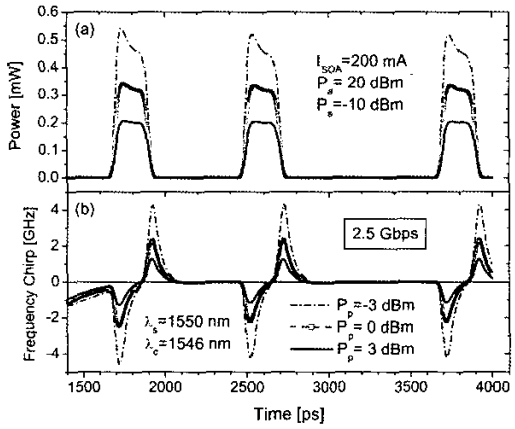

Fig. 4. The output conjugate pulse and the frequency chirp of the proposed wavelength converter scheme at I=200 mA (at gain region).

indicating the slowing of the response as the device is operated at lower biases. The increased carrier lifetime is in close relation to the saturation power of a SOA as shown in Fig. 2. For wavelength conversion, both the SOA gain and saturation power need to be as high as possible. When a shorter wavelength holding light is used, however, the SOA can be operated at a higher bias level and still provide transparency to the holding light (Fig. 2). In other words, using a shorter wavelength holding light can provide the improvements at higher gain and obtain a superior dynamic performance.

B. Extinction Ratio

Fig. 5(a) shows the effect of varying the signal input optical power on the dynamic performance, whilst keeping all other operating parameters constant. Here, we set the extinction ratio of the input signal to 10 dB (high: -10 dBm; low: -20 dBm). It is clearly seen that as the input signal power increases, the peak chirp increases, at the expense of extinction ratio. The extinction decreases after wavelength conversion since lower signal power level has higher conversion efficiency than higher signal power level, as shown in Fig. 2.

Fig. 5(b) shows the effect of varying the holding light power on the conversion dynamics. Although conversion speed and efficiency of the SOA are improved, the extinction ratio of the conjugate signal remains unchanged as we increase the holding light power. In addition, the peak chirp increases according to the increase in the holding light power. However, injecting an assist light can effectively increase the conversion efficiency; and the larger the assist light power, the more the conversion efficiency improves.

The assist light does not cause any perturbation in the active layer in the steady state, since the gain is zero. In the presence of the signal light, excess carriers are not transported but radiatively recombined in the active layer by the assist light. Thus, there is no carrier transport and heat generation process,

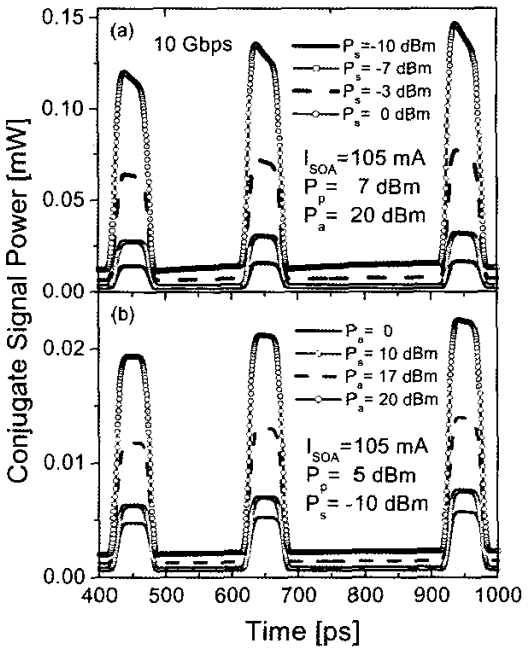

Fig. 5. The output conjugate pulse of the proposed wavelength converter scheme with various (a) various input signal powers and (b) assist light powers at I=105 mA (at transparency).

which is an advantageous feature in handling high repetition rate signals as well as ultrashort pulses.

Fig. 6 shows extinction ratio of output conjugate signal with the extinction ratio of 10 dB for the input signal. Extinction ratio decreases with the pump power decreases and the signal power increases. In other words, when either pump power or signal power is fixed, extinction ratio decreases with the decreasing pump-to-signal (P/Q) ratio. It results from smaller difference of conversion efficiency between low signal power level and high signal power level at low P/Q ratio than at high P/Q ratio.

C. Peak Frequency Chirp

Peak frequency chirp occurs during wavelength conversion inside SOA's, which is responsible for refractive index modulation by carrier density variation. Peak frequency chirp can obstruct the perfect compensation for GVD and SPM. Fig.7 shows peak frequency chirp of output conjugate signal as a function of input pump power. Peak frequency chirp is minimized at higher P/Q ratio. By definition, frequency chirping is a monotonically increasing function of the linewidth enhancement factor (α_c) and the extinction ratio [14]. In our scheme, the injection of a holding light enhances the FWM conversion efficiency but degrades the output extinction ratio. However, the frequency chirping actually comes to increase. On the other hand, the α-parameter is a key parameter in obtaining low-chirp emission from high-speed directly modulated lasers.

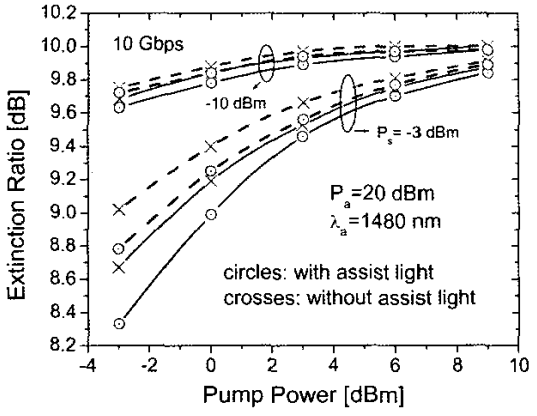

Fig. 6. Extinction ratio as a function of pump power with different average input signal power (extinction ratio of input signal = 10 dB, λ_s=1550 nm, λ_c=1546 nm). Solid and dashed lines represent the SOA with injection currents of 120 and 105 mA, respectively.

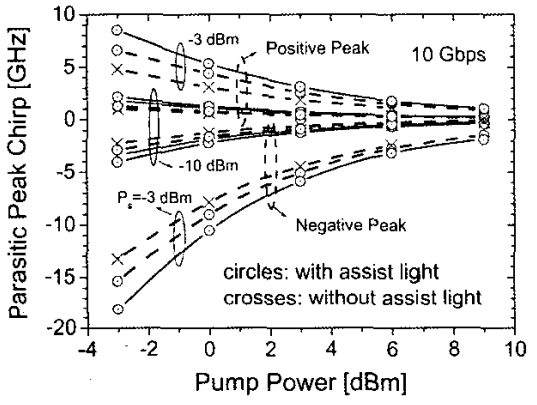

Fig. 7. Peak frequency chirp as a function of pump power with different average input signal power (extinction ratio of input signal = 10 dB, λ_s=1550 nm, λ_c=1546 nm). Solid and dashed lines represent the SOA with injection currents of 120 and 105 mA, respectively.

Hence, lasers with lower values of α_c (ex. quantum dot lasers) should exhibit lower frequency chirp under high-speed modulation. Resorting to this result, and in combination with our novel scheme, we could thus develop a high-efficiency and low-chirp wavelength converter based on FWM in a quantum dot laser amplifier [15].

V. Conclusion

We have proposed and investigated a new wavelength converter using a SOA and a CW-holding light. The effect of holding light on the static characteristics and dynamic performance in the new scheme has been considered. Our simulation method took into account FWM, ASE noise, longitudinally variation of the carrier density due to spatial hole burning, wavelength dependent gain and extinction ratio of input signal power. It is shown that the conversion efficiency can be improved by larger than 6 dB when the SOA is biased at the transparent current for 20 dBm of 1480-nm holding light. High-pump power can contribute to maximize extinction ratio and minimize parasitic frequency chirp. Under our scheme, through the injection of a shorter wavelength holding light, we can provide performance improvements at higher gain, which is needed for high-efficiency and low-noise FWM wavelength conversion.

Acknowledgment

Part of this work is supported by the National Science Council and the Ministry of Education, Taiwan, R.O.C. under Grants NSC91-2215-E-011-001 and 89E-FA06-2-4-7.

References

[1] D. F. Geraghty, R. B. Lee, M. Verdiell, M. Ziari, A. Mathur, and K. J. Vahala, "Wavelength conversion for WDM communication systems using four-wave mixing in semiconductor optical amplifiers," *IEEE J. Select. Topics Quantum Electron.*, vol. 3, pp. pp. 1146-1155, Oct. 1997.

[2] S. J. B. Yoo, "Wavelength conversion technologies for WDM network applications," *IEEE Journal of Lightwave Technology*, vol.14, pp.955-966, 1996.

[3] A. D'Ottavi, F. Girardin, L. Graziani, F. Martelli, P. Spano, A. Mecozzi, S. Scotti, R. Dall'Ara, J. Eckner, G. Guekos, "Four-wave mixing in semiconductor optical amplifiers: a practical tool for wavelength conversion", *IEEE J. Select. Topics Quantum Electron.*, vol.3, pp.522-528, 1997.

[4] M. A. Dupertuis, J. L. Pleumeekers, T. P. Hessler, P. E. Selbmann, B. Deveaud, B. Dagens, and J. Y. Emery, "Extremely fast high-gain and low-current SOA by optical speed-upat transparency," *IEEE Photon. Technol. Lett.*, Vol.12, pp.1453-1455, 2000.

[5] M. Usami, M. Tsurusawa, and Y. Matsushima, "Mechanism for reducing recovery time of optical nonlinearity in semiconductor laser amplifier," *Appl. Phys. Lett.*, Vol. 72, pp. 2657-2659, 1998.

[6] S. L. Lee, P. M. Gong, and C. T. Yang, "Performance Enhancement on SOA-Based Four-Wave-Mixing Wavelength Conversion Using an Assisted Beam", *IEEE Photon. Technol. Lett.*, vol. 14, pp. 1713-1715, 2002.

[7] N. Storkfelt, B. Mikkelsen, D. S. Olesen, M. Yamaguchi, and K. E. Stubkjaer, "Measurement of carrier lifetime and linewidth enhancement factor for 1.5-μm ridge-waeguide laser amplifier," *IEEE Photon. Technol. Lett.*, Vol. 3, 162-164, 1991.

[8] A. E. Willner and W. Shieh, "Optimal spectral and power parameters for all optical wavelength shifting: Single stage, fanout, and cascadability," *J. Lightwave Technol.*, vol. 13, pp. 771-781, May 1995.

[9] Y. Suematsu and A. R. Adams, *Handbook of Semiconductor Laser and Photonic Integrated Circuits*, London: Chapman & Hall, 1994.

[10] G. P. Agrawal and N. K. Dutta, *Semiconductor Lasers*. New York: Van Nostrand, 1993.

[11] J. Zhou, N. Park, J. W. Dawson, K. J. Vahala, M. A. Newkirk, and B. I. Miller, "Efficiency of broadband four-wave mixing wavelength conversion using semiconductor traveling-wave amplifiers," *IEEE Photon. Technol. Lett.*, Vol. 6, pp. 50-52, Jan. 1994.

[12] A. J. Lowery, "Amplified spontaneous emission in semiconductor laser amplifiers: Validity of the transmission line laser model," *Proc. Inst. Elect. Eng.*, pt. J, vol. 137, pp. 241-247, Aug. 1990.

[13] T. Mukai, Y. Yamamto, and T. Kimura, "S/N and error rate performance in AlGaAs semiconductor laser preamplifier and linear repeater systems," *IEEE Trans. Microwave Theory Tech.*, vol. 30, pp. 1548-1556, 1982.

[14] T. L. Koch and R. A. Linke, "Effect of nonlinear gain reduction on semiconductor laser wavelength chirping," *Appl. Phys. Lett.*, vol. 48, no. 10, pp. 613-615, Mar. 10, 1986.

[15] S. Ghosh, S. Pradhan, and P. Bhattacharya, "Dynamic characteristics of high-speed $In_{0.4}Ga_{0.6}As$/GaAs self-organized quantum dot lasers at room temperature," *Appl. Phys. Lett.*, vol. 81, pp. 3055-3057, 2002.